



# MATERIALS AND METHODS FOR LARGE-AREA SOLAR CELLS

by

S. G. Ellis (Project Engineer), R. R. Addiss, E. F. Pasierb,  
R. S. Silver, and P. Vohl

prepared for

NATIONAL AERONAUTICS AND SPACE ADMINISTRATION

CONTRACT NAS 9-2796



RADIO CORPORATION OF AMERICA  
RCA LABORATORIES  
PRINCETON, NEW JERSEY

NOTICE

This report was prepared as an account of Government sponsored work. Neither the United States, nor the National Aeronautics and Space Administration (NASA), nor any person acting on behalf of NASA:

- A.) Makes any warranty or representation, expressed or implied, with respect to the accuracy, completeness, or usefulness of the information contained in this report, or that the use of any information, apparatus, method, or process disclosed in this report may not infringe privately owned rights; or
- B.) Assumes any liabilities with respect to the use of, or for damages resulting from the use of any information, apparatus, method or process disclosed in this report.

As used above, "person acting on behalf of NASA" includes any employee or contractor of NASA, or employee of such contractor, to the extent that such employee or contractor of NASA, or employee of such contractor prepares, disseminates, or provides access to, any information pursuant to his employment or contract with NASA, or his employment with such contractor.

Requests for copies of this report should be referred to  
National Aeronautics and Space Administration  
Office of Scientific and Technical Information  
Attention: AFSS-A  
Washington, D.C. 20546

CASE FILE COPY

**MIDPOINT REPORT**

**MATERIALS AND METHODS FOR LARGE-AREA SOLAR**

*by*

**S. G. Ellis (Project Engineer), R. R. Addiss, E. F. Pasierb,  
R. S. Silver, and P. Vohl**

***Approved by: P. Rappaport (Project Supervisor)***

*prepared for*

**NATIONAL AERONAUTICS AND SPACE ADMINISTRATION**

**April 20, 1964**

**CONTRACT NAS 3-2796**

**Technical Management  
NASA Lewis Research Center  
Cleveland, Ohio  
Space Power Systems Office  
Andrew Potter**



**RADIO CORPORATION OF AMERICA  
RCA LABORATORIES  
PRINCETON, NEW JERSEY**

## TABLE OF CONTENTS

<u>Section</u>	<u>Page</u>
List of Illustrations . . . . .	iv
Purpose . . . . .	v
Abstract . . . . .	v
I. Gallium Arsenide Films . . . . .	1
II. Barriers . . . . .	7
III. Cu <sub>2</sub> S Preparation and Properties . . . . .	9
IV. Cells . . . . .	12
V. I-V Characteristics . . . . .	14
VI. Photoangular Effect . . . . .	18
VII. Other Studies . . . . .	23
Conclusions . . . . .	27
Future Plans . . . . .	28

## LIST OF ILLUSTRATIONS

<u>Figure</u>	<u>Page</u>
1. $V_{oc}$ :position for p-n junction in melt-grown polycrystalline GaAs . . . . .	2
2. $V_{oc}$ :position along line AA'. The effect of etching . . . . .	2
3. A photomicrograph of part of the crystal under study . . . . .	4
4. Specific resistivity: thickness for evaporated $Cu_2S$ films treated over ammonium sulphide . . . . .	9
5. Optical transmission: sheet conductivity for $Cu_2S$ on glass . . .	10
6. Optical transmission spectra of $Cu_2S$ films on glass . . . . .	11
7. I-V characteristic for cell #299 under illumination . . . . .	12
8. I-V characteristic for cell #298 under illumination . . . . .	13
9. Forward I-V characteristic for $Cu_2S$ on single crystal GaAs . . .	14
10. Forward I-V characteristic for $Cu_2S$ on polycrystalline GaAs film . . . . .	16
11. Drawing to illustrate definitions of $\theta$ and $\emptyset$ . . . . .	19
12. Variation of photovoltage with $\theta$ . . . . .	20
13. Variation of photovoltage with temperature . . . . .	21
14. Spectral response of photoangular effect . . . . .	22
15. Optical transmission spectra for GaAs film sputtered onto glass . . . . .	24

## PURPOSE

The purpose of the program is to investigate materials and methods for the fabrication of large-area solar cells. The aims of this program are to have efficiencies higher than 5 percent, areas of the order of one foot square, flexible cells, and relatively inexpensive production costs.

## ABSTRACT

20671

A

The preparation and properties of  $\text{Cu}_2\text{S}$  layers have been studied in detail.  $\text{Cu}_2\text{S}$  on polycrystalline GaAs films have yielded solar cells approaching  $1\text{ cm}^2$  in size with 1.5% sunlight efficiency. This is limited by the poor compromise between sheet resistance and optical transparency that  $\text{Cu}_2\text{S}$  enforces. Detailed measurements of the V-I characteristics and the variation of junction capacitance with voltage for  $\text{Cu}_2\text{S}$  on single-crystal GaAs diodes have been made. They are electrically indistinguishable from metal-semiconductor barriers at present. A new photovoltaic effect has been found in some semiconductor films. In this effect the photovoltage increases as the angle of illumination departs from the normal to the film. Voltages higher than bandgap have been observed. A start has been made on both the sputtering, and fast flash-evaporation of GaAs.

Author

## I. GALLIUM ARSENIDE FILMS

It was shown in previous work<sup>\*</sup> that if a p-n junction is made on a polycrystalline GaAs film either by growth or diffusion, the junction shows leakage. Three possible causes have been advanced:

- (a) Due to the high temperatures and long times involved in the junction preparation, diffusion has taken place along some grain boundaries, thus causing a short circuit to the metal substrate.
- (b) Cracks in the film have caused short-circuiting.
- (c) The grain boundaries are inherent leakage paths (for example, they may always have inversion layers associated with them).

Since the grain boundaries in the films are too close together to make this study easy some melt-grown n-type GaAs polycrystals were obtained. These were approximately 1 cm x 2 cm in size and had been Zn-diffused to produce a p-type layer approximately 2 microns thick on one face. The crystal had an ohmic contact all over the n-type face and, as supplied, was unetched.

One of these polycrystals was mounted so that the p-type face could be uniformly illuminated and a fine gold probe (connected to a high-impedance amplifier) was pulled across the face.  $V_{oc}$  was then recorded on an x-y recorder as a function of the probe position. By repeating this on parallel paths 1 mm apart a "map" of the variation of  $V_{oc}$  over the p-type face was obtained. The results of three such traces are shown in Fig. 1.

Subsequently, the p-type face was etched repeatedly with a slow etch, and the "mapping" procedure was performed after each etching. The etching procedure was stopped when the p-type region had been etched through at one region. Traces along the line A-A' are shown after the first, 13th, and 18th etches in Fig. 2.

The results and some of the conclusions may now be summarized:

- (i) Most of the intercrystalline boundaries do not form low-impedance paths between the n- and p-type regions. They do provide some addition to the sheet resistance of the p-type layer.

---

<sup>\*</sup> First Quarterly Report, Dec. 31, 1962, p. 6, Contract No. NAS 7-202.

Fourth Quarterly Report, Oct. 30, 1963, p. 14, Contract No. NAS 7-202.

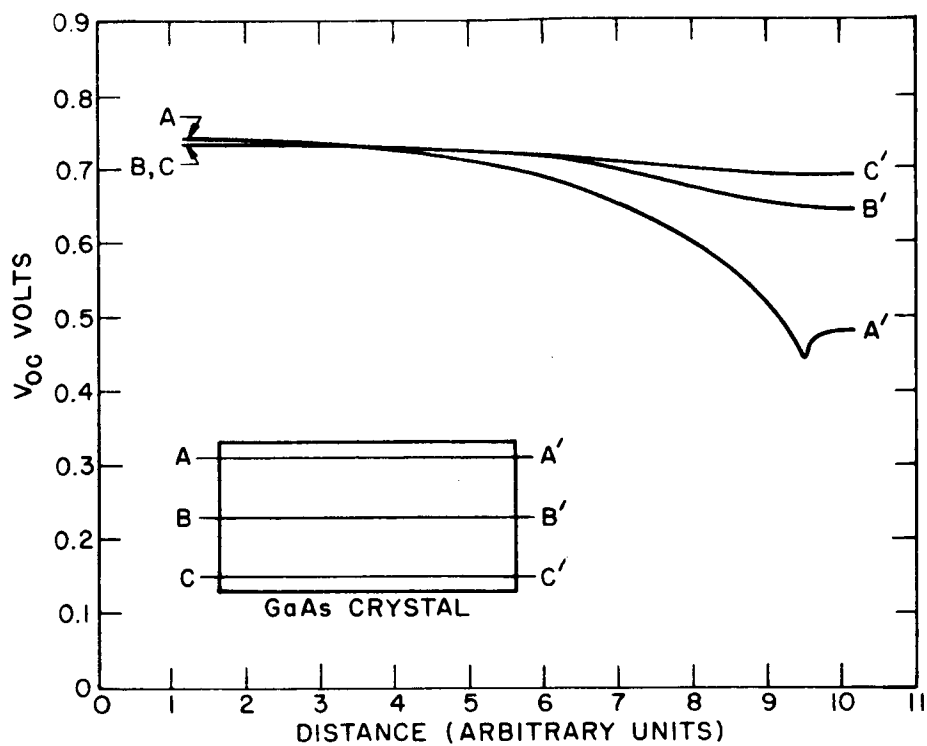


Fig. 1.  $V_{OC}$ : position for p-n junction in melt-grown polycrystalline GaAs.

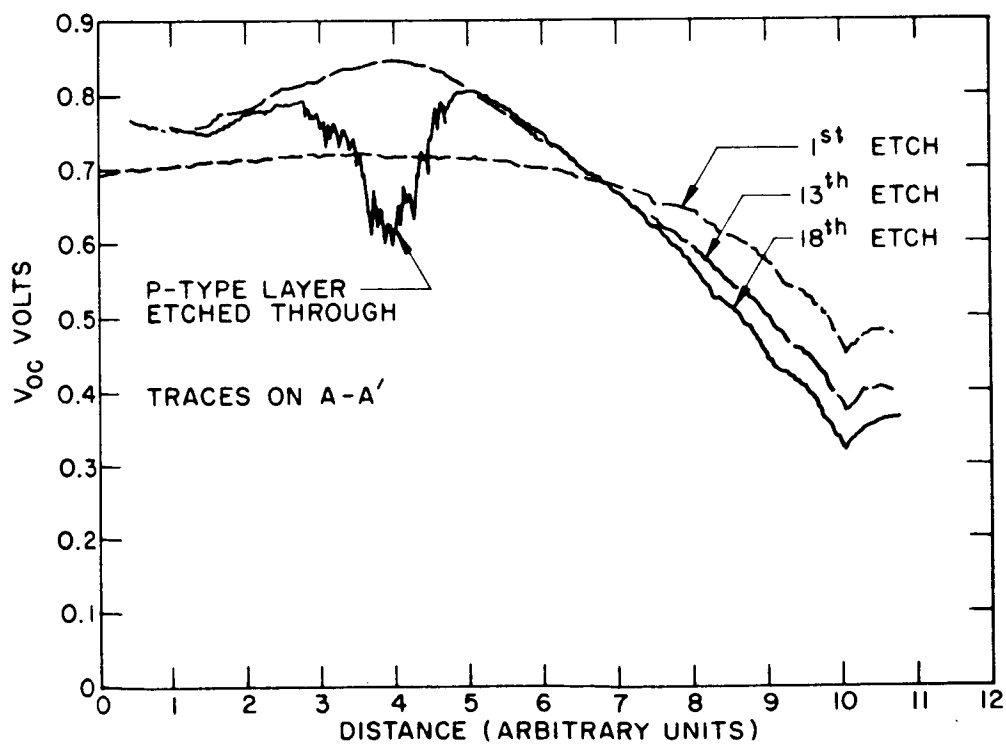


Fig. 2.  $V_{OC}$ : position along line AA'. The effect of etching.



- (ii) In the first polycrystal studied, there is one highly localized defect which reduces  $V_{oc}$  in its vicinity.
- (iii) An I-V characteristic taken at places of high  $V_{oc}$  (after etching) showed good rectification. An I-V characteristic taken near the defect was almost linear, showing that the defect is a low-impedance path across the junction.
- (iv) Before etching,  $V_{oc}$  is 0.4 volt near this low-impedance path and 0.7 volt at places remote from it.
- (v) After etching, which reduces the junction depth and increases the sheet resistance,  $V_{oc}$  eventually increases to 0.8 volt away from the defect, but is reduced to 0.3 volt near the defect. The effect of the low-impedance path is more localized in the sense that the gradient of  $V_{oc}$  in the p-type surface is higher, but  $V_{oc}$  is still down to 0.55 volt at 3 mm from the path.

The magnification between the probe-moving apparatus and the x-y recorder was measured. The  $V_{oc}$  distance traces then provided approximate coordinates for the location of the defect in the polycrystal. In Fig. 3, which is a photomicrograph of part of the polycrystal, the rectangle surrounds the defect and by the length of its sides shows the uncertainty in the measurements of position.

A second polycrystalline wafer showed a similar distribution of inter-crystalline boundaries and was evidently cut from the same ingot. It, too, showed a low-impedance path shorting the junction at or near the same juncture of three crystal boundaries. It seems unlikely therefore that the short-circuiting is caused by a point-defect at the junction, but rather that it is associated with the linear crystallographic mismatch at this triple boundary.

In a continuation of this work the p-type layer was removed from the first wafer by grinding, and after suitable etching  $Cu_2S$  was evaporated down in its place. The usual rectification and photovoltaic response (see the section on Barriers) was observed, but in this case no leakage was observed. It must be noted, however, that during the processing the large-area ohmic contact to the n-type side had been removed and replaced by small-area contacts, none of which was in contact with the triple boundary.

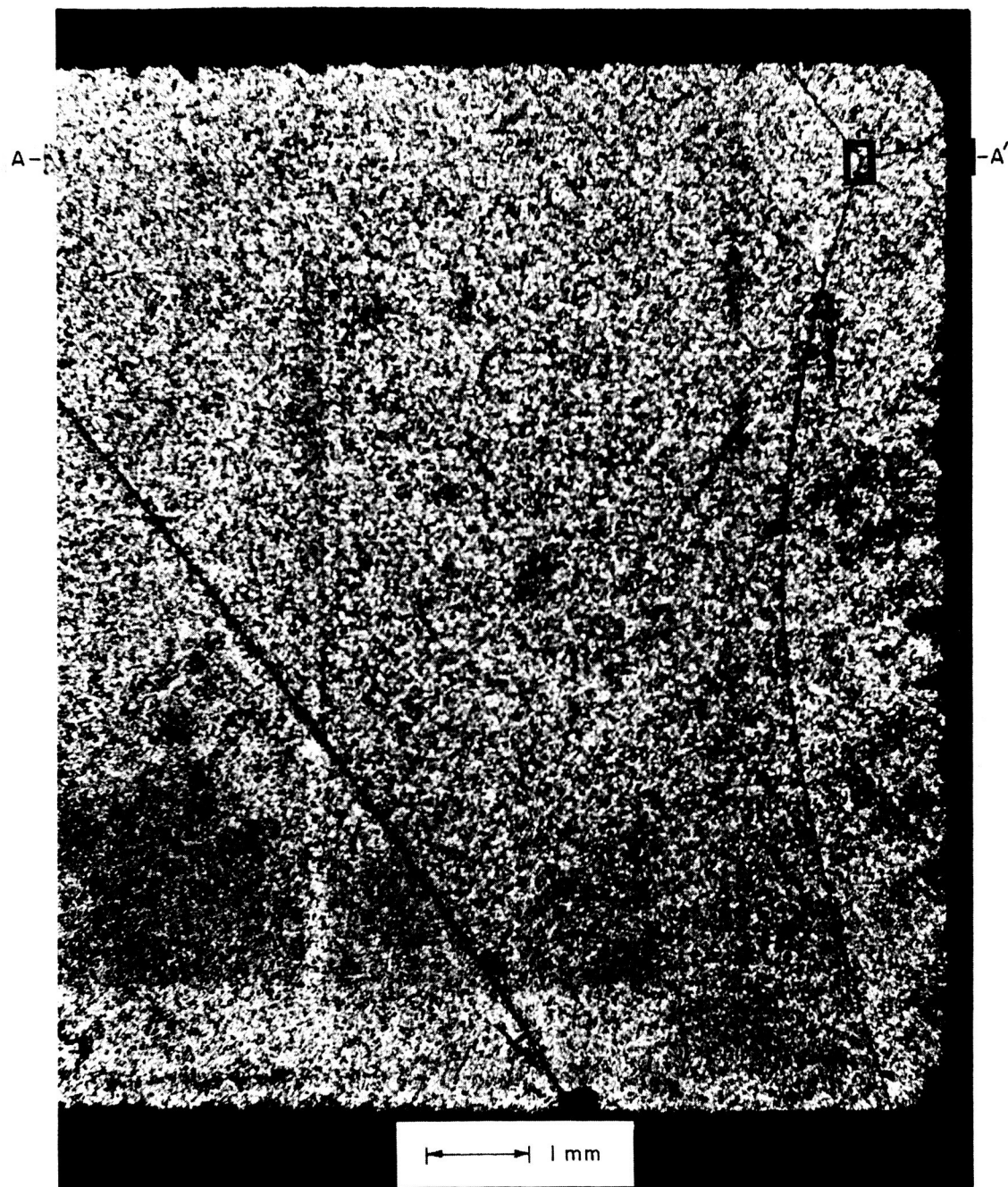


Fig. 3. A photomicrograph of part of the crystal under study.

The chief conclusions to be drawn from these experiments are that during the Zn diffusion the penetration was very far down one particular crystal defect. While the small number of such defects in the melt-grown crystals and the very large number of defects in the transport-grown layers

make statistical comparisons uncertain, it is probably accurate to state that diffusions (or crystal growth of opposite-conductivity-type layers) involving temperatures of the order of 700°C for ten or more minutes are ruled out for making polycrystalline large-area cells.

While in these experiments there was no strong evidence for the grain boundaries being inherent leakage paths, it must be remembered that a small effect in this direction might become prominent in polycrystalline films where the numbers of grain boundaries per  $\text{cm}^2$  is of the order  $10^4$  times higher.

When a GaAs film is cooled from the growth temperature, it contracts more than the Mo or W substrate and is therefore placed in tension. The square substrate bows to a cylindrical form, giving partial stress relief in one direction. The residual stress increases the fragility of the structure and, if it is mishandled, the film can crack or separate from the substrate, sometimes in one piece. Cracks caused in this way are readily detected.

A more subtle form of cracking can be seen if a carefully handled film is examined under the light microscope. It appears as an irregular network of fine lines, of the order of one millimeter apart whose course is independent of the grain boundaries. The reasons for calling these lines cracks are their appearance at high magnification and the fact that they etch through more rapidly than the rest of the film.

There is some doubt that these fine cracks penetrate all the way through the film. When a film is flaked off its substrate it does not break into millimeter-sized pieces, and the cracks usually cannot be seen on the smooth side of the film that was in contact with the substrate.

The appearance of these cracks has not changed with changes in substrate (W, Mo, Ge on Mo, quartz), temperature during deposition, substrate thickness, or film thickness. More surprisingly, these cracks have been seen on a film grown on a previously made GaAs film used as substrate. While unsatisfactory, the presence of these small cracks does not seem to preclude making diodes by evaporation processes. It may be that the cracks do not, in general, face the evaporator source and that any part of an evaporated film that penetrates a crack to the substrate is too thin (because of oblique deposition on the walls of the crack) to cause a serious short.

An attempt has been made to estimate the carrier concentration of n-type films by comparing the reverse breakdown voltage (i.e., the voltage at which the reverse current becomes 1 or 2  $\mu\text{a}$ ) for Au on films and crystals of known carrier concentration. In a separate study, the variation of junction capacitance with voltage for  $\text{Cu}_2\text{S}$  on films and crystals was compared. The results are rough because the form of the characteristic is different for the film and single crystals. Both methods, however, gave carrier concentrations in the high  $10^{17} \text{ cm}^{-3}$  range.

## II. BARRIERS

The general considerations governing this work were given in the Fourth Quarterly Report, dated October 30, 1963, page 2.\* In the intervening period we have continued to search for new barrier-forming materials (without conspicuous success), and have studied the formation of barriers with cuprous sulphide in more detail. The preparation and properties of cuprous sulphide films are described in the next section.

The results of the search for new barrier-forming materials are summarized in Table I, for those materials which were expected to be evaporable. In most cases, post-evaporative chemical treatments were tried without improvement in the results.

TABLE I  
New Barrier-Forming Materials

Material Evaporated	Results	Comments
Bi <sub>2</sub> O <sub>3</sub>	V <sub>oc</sub> = 0.15 volt    η low	V <sub>oc</sub> too low for good efficiency
MoO <sub>3</sub>	—	Sheet resistance >10 <sup>8</sup> ohms/square
NiO	—	Decomposed before evaporation
PbO	—	Decomposed before evaporation
NiS	—	Decomposed before evaporation
SnS	Small photovoltaic effect	Sheet resistance — 10 <sup>7</sup> ohms/sq. Band gap — 1.07 eV
Cu <sub>3</sub> P	V <sub>oc</sub> = 0.4 v, I <sub>sc</sub> = 260 μa, η ≈ 1.5%	No better than Cu <sub>2</sub> S

Since brasses can be electroplated, some layers were plated onto n-GaAs single crystal and were subsequently exposed to the vapor over ammonium sulphide. Plating or subsequent chemical treatments did not improve the performance over that of a "pure" Cu<sub>2</sub>S/GaAs barrier.

\* Contract No. NAS 7-202.

Electroplating was also used to deposit a layer of  $\text{Ni}_3\text{S}_2$ . As plated, it gave:  $V_{oc} = 0.15$  v,  $I_{sc} = 0.7$  ma with a focussed microscope light, but the sheet resistance was too high for acceptable efficiency.

Cuprous selenide, as evaporated, is probably n-type since it makes an ohmic contact to n-type GaAs. After treatment with air or  $\text{H}_2\text{S}$ , it becomes p-type and gives barriers not markedly different from those reported in the Fourth Quarterly Report.\*

From what is known of the post-evaporative treatment of  $\text{Cu}_2\text{S}$  layers (see the next section) it appears that the treatments used on  $\text{Cu}_2\text{Se}$  layers may not be ideal.

Barriers have been formed on n-GaAs single crystals by the vacuum deposition of  $\text{Cu}_2\text{Te}$ . This is simpler than the electrochemical method.\* The reverse impedance of these barriers has been low, however, and the sheet resistance of the  $\text{Cu}_2\text{Te}$  layer high.

---

\* See the Fourth Quarterly Report, Contract No. NAS 7-202, dated October 30, 1963.

### III. $\text{Cu}_2\text{S}$ PREPARATION AND PROPERTIES \*

Cuprous sulphide, as prepared chemically, conducts because of the acceptor property of the Cu vacancies. The formula is sometimes written  $\text{Cu}_{2-x}\text{S}$  with  $x$  as high as 0.2. It is usually obtained as a black powder, and it is desirable to sinter or pre-melt this under continuous evacuation in a quartz tube to obtain a charge for the vacuum evaporator which will not fly out of the heater. Sulphur is lost in this preliminary firing.

In the vacuum evaporation, the charge is melted with a shutter between it and the substrate. During this time the pressure rises and then falls. When it has stabilized, the shutter is opened and the deposition proceeds at rates on the order of  $10 \text{ \AA}/\text{sec}$  for a source-to-substrate distance of 7 cm. Attempts to monitor the film thicknesses by measuring resistance across the films lead to irregular results, and the optical density of the film is now used for monitoring purposes. The charge can be reused but may have to be driven to a higher temperature in further evaporations.

The specific resistance of the  $\text{Cu}_2\text{S}$  films immediately upon exposure to air is 200 ohm-cm. Upon continued exposure to air, this value will drop with time by a factor which is bigger for the thinner films. Indeed, the thinnest films had the lowest resistance. This reaction can be accelerated by heating. Air-heated films are not stable (resistance-wise) to heating and moisture.

If the freshly evaporated films are exposed immediately to the vapor over ammonium sulphide, the resistivity drops to a value of approximately  $6.5 \times 10^{-4}$  ohm-cm, which is nearly independent of film thickness (see Fig. 4). This

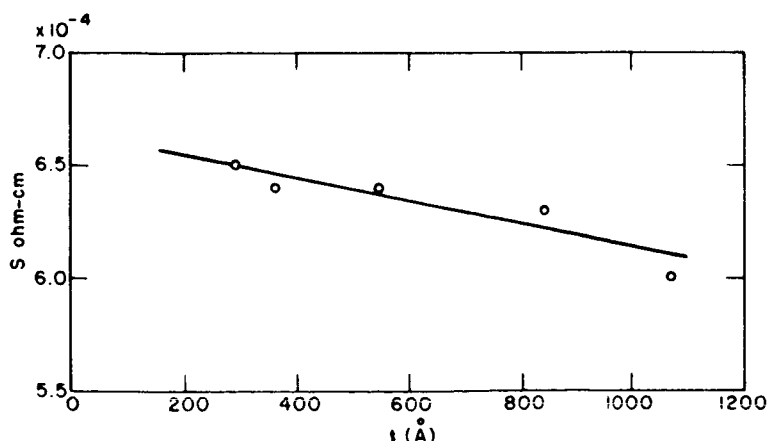


Fig. 4. Specific resistivity: thickness for evaporated  $\text{Cu}_2\text{S}$  films treated over ammonium sulphide.

\* Not all of the work reported in this section was done under this contract.

reaction is fast and, even for films 3000 Å thick, is completed in less than 2 minutes at room temperature. Films heated this way are stable to moisture and to heating to 200°C in air.

Figure 5 shows the variation of light transmission with sheet conductivity for  $\text{Cu}_2\text{S}$  films evaporated onto glass and treated with ammonium sulphide vapor. The distribution of points suggests that the  $\text{Cu}_2\text{S}$  films may be acting in part as an antireflection coating.

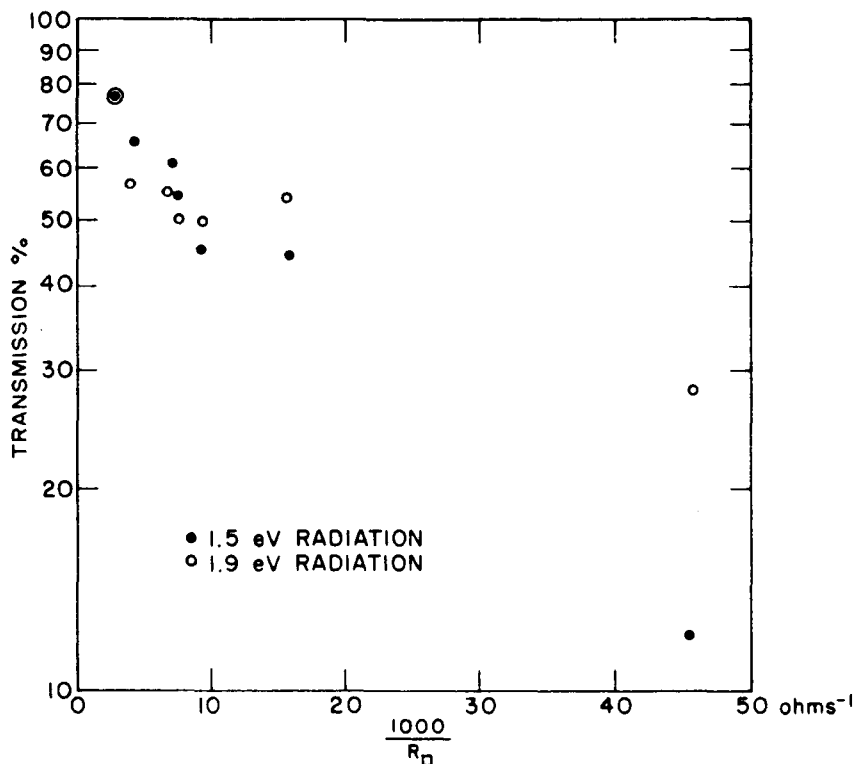


Fig. 5. Optical transmission: sheet conductivity for  $\text{Cu}_2\text{S}$  on glass.

The optical transmission spectrum of an as-deposited  $\text{Cu}_2\text{S}$  film is shown in Fig. 6 (curve a). The absorption edge indicates an optical bandgap in the neighborhood of 1.5 eV ( $\pm 0.2$  eV). There is also some indication that an impurity level may exist in the neighborhood of 0.7 eV from the band edge. The optical transmission spectrum for a film after ammonium sulphide treatment is also shown in Fig. 6 (curve b). The absorption edge indicates an apparent bandgap between 1.8 and 2.0 eV; there is also an absorption band in the infrared, beginning at about 1.8 eV and increasing with decreasing photon energy.



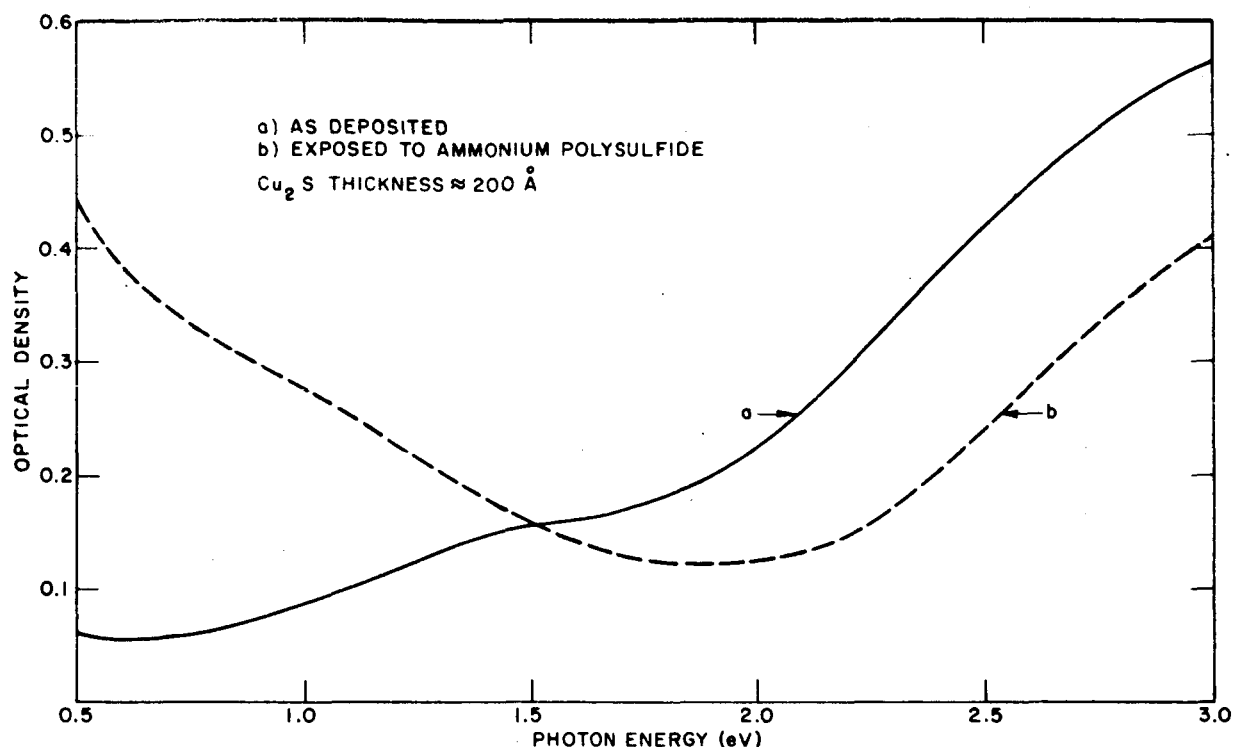


Fig. 6. Optical transmission spectra of  $\text{Cu}_2\text{S}$  films on glass.

These results can be interpreted tentatively as follows. Upon reducing the resistivity by forming a high concentration of Cu ion vacancies, the material becomes degenerate. Therefore, the Fermi level lies below the valence band edge (p-type conductivity) and a higher photon energy is needed to excite electrons from the Fermi level to the conduction band edge than was previously required to excite electrons from the valence band edge to the conduction band edge; thus, an apparently higher bandgap is observed. The high concentration of free carriers in the degenerate material gives rise to free carrier absorption in the near infrared.

With regard to forming a photovoltaic barrier on n-type GaAs, the advantage of exposing the  $\text{Cu}_2\text{S}$  layer to ammonium polysulfide is twofold. Not only is the resistivity drastically reduced, but there is also a net gain in the light transmitted to the GaAs for those wavelengths to which the GaAs is sensitive (energies above 1.4 eV).

#### IV. CELLS

A few cells have been made with the aim of obtaining sunlight efficiencies. Cell 299 is a fair example. It consists of a 1 cm x 1 cm n-GaAs film on molybdenum. The original film thickness was 3 mils (by weight). The film was etched for a few minutes in  $4\text{H}_2\text{SO}_4$ ,  $1\text{H}_2\text{O}_2$ ,  $1\text{H}_2\text{O}$  to make it smoother. Immediately before insertion into the vacuum evaporator it was etched with bromine-alcohol, then alcohol-washed and dried. The  $\text{Cu}_2\text{S}$  film is approximately 9 mm x 8 mm, and on this a gold strip 7 mm x 0.25 mm was centrally deposited after the ammonium sulphide treatment.

The I-V characteristics of this and a similar cell are shown in Figs. 7 and 8. These were taken on a solar simulator set to give a value of  $I_{sc}$  which had been determined by sunlight irradiation.

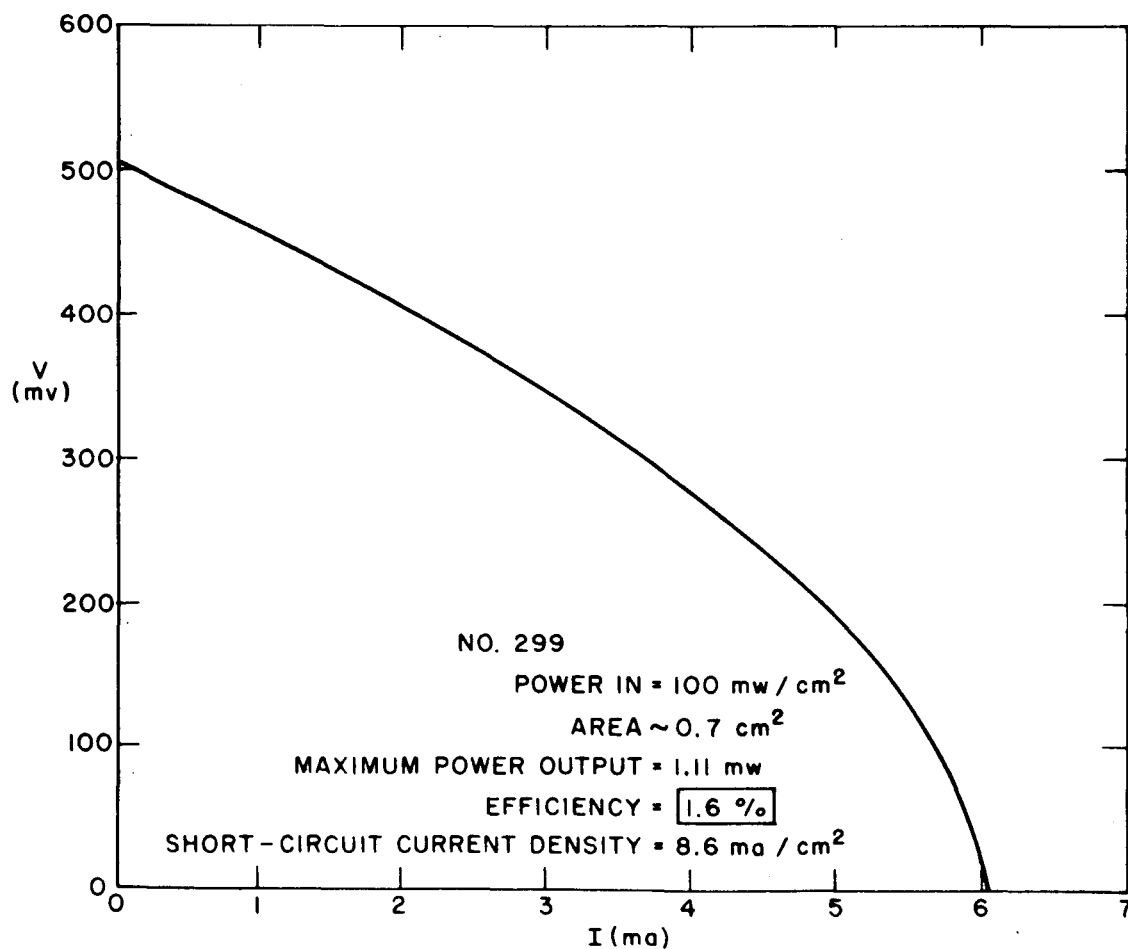


Fig. 7. I-V characteristic for cell 299 under illumination.

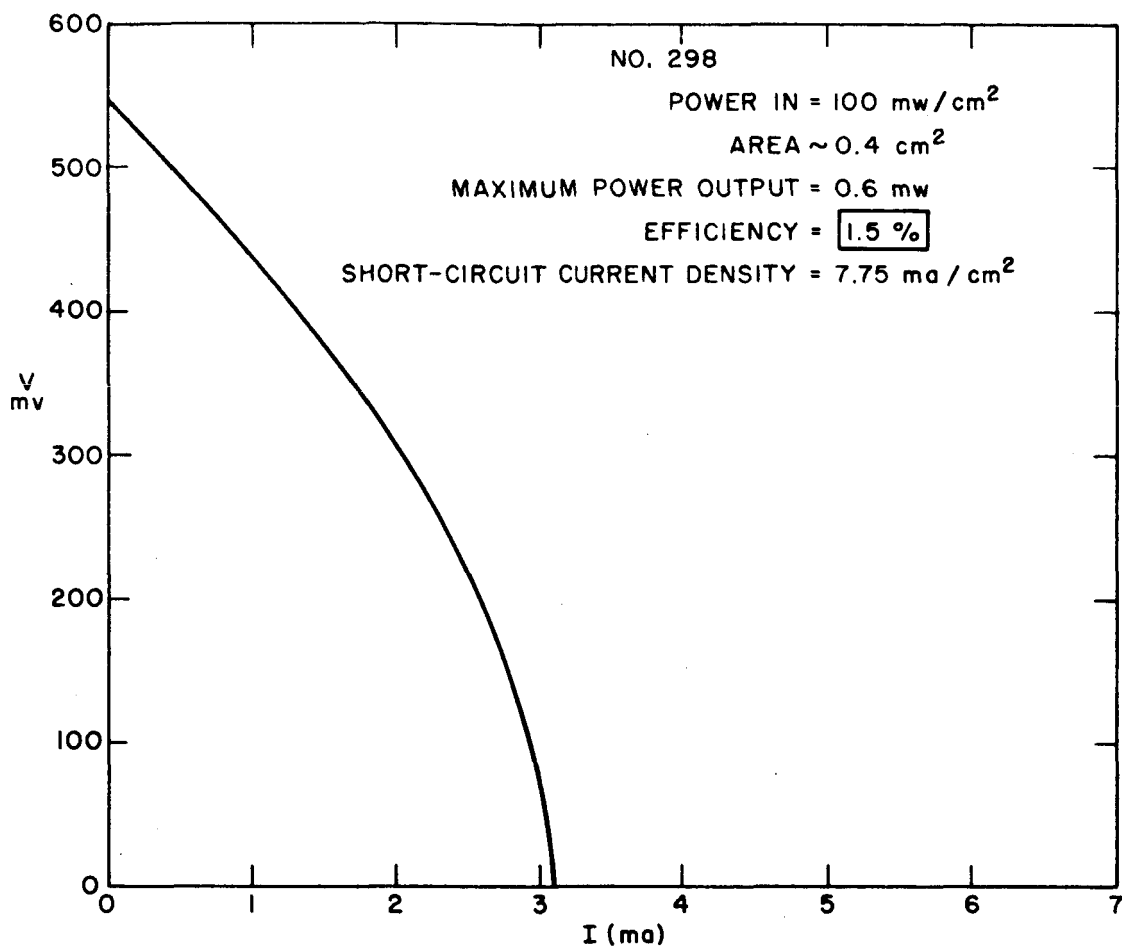


Fig. 8. I-V characteristic for cell #298 under illumination.

We find  $V_{oc} \approx 0.5$  volt, short-circuit current density  $\approx 8$  ma/cm<sup>2</sup>, and  $\eta_{sun} \approx 1.5\%$ . The Cu<sub>2</sub>S films were approximately 60% transmitting and the effect of sheet resistance is evident.

Of four such cells made to date, two were shorted. One film showed a crack due to mishandling. The source of the other short is unknown.

## V. I-V CHARACTERISTICS

### A. DEFINITION OF OPERATIONAL PARAMETERS

Measurements of  $I$  vs.  $V$  on  $\text{Cu}_2\text{S}$  barrier diodes (fabricated on single crystal and polycrystalline GaAs) indicate that the generalized diode equation:

$$I = I_x (e^{qv/\alpha kT} - 1)$$

is not sufficient to describe the characteristics of these diodes. Figure 9 illustrates a  $\ln I$  vs.  $V$  characteristic for a typical diode on single crystal

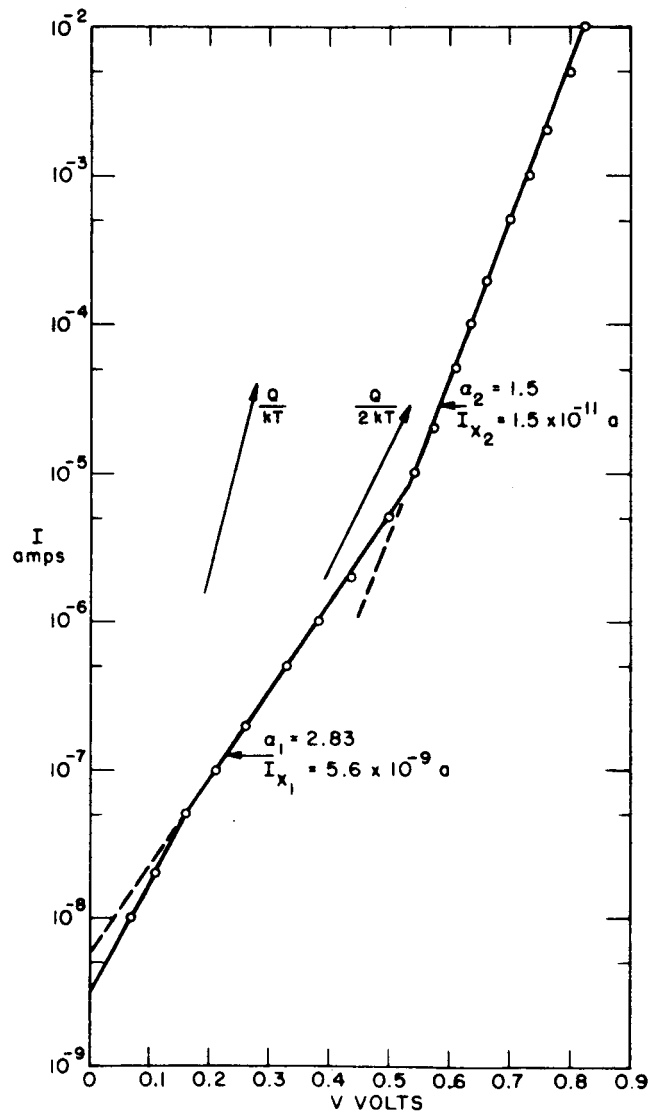


Fig. 9. Forward I-V characteristic for  $\text{Cu}_2\text{S}$  on single crystal GaAs.

GaAs. It is apparent that an effective  $I_x$  and  $\alpha$  may be defined for each of the two linear portions of the characteristic. The parameters  $I_x$  and  $\alpha$  are defined operationally as: The slope of the  $\ln I$  vs.  $V$  characteristic in each linear region defines an effective  $\alpha$ ; the intersection of the extrapolated tangent to each "linear" region with the  $\ln I$  axis defines an effective  $I_x$ .

## B. TABULATION OF DATA

A summary of data obtained on prepared devices appears in Table II. Figure 10 illustrates the  $\ln I$  vs.  $V$  characteristic for a typical diode on polycrystalline GaAs. Since this device has only one "linear" region in its characteristic, only one value of  $I_x$  and  $\alpha$  may be defined.

TABLE II  
SUMMARY OF DATA ON PREPARED DEVICES

Sample	Donor Density ( $\text{cm}^{-3}$ )	Saturation Current Density $I_x/\text{Area} - \text{amp cm}^{-2}$	$\alpha_2$
P-N Junction			
G-260	$5.2 \times 10^{17}$	$3 \times 10^{-8}$	2.33
G-328	$9.4 \times 10^{17}$	$8 \times 10^{-6}$	4.0
G-232	$6.3 \times 10^{16}$	$6 \times 10^{-10}$	2.0
G-94	$2.9 \times 10^{17}$	$8 \times 10^{-9}$	2.16
Metal-Semiconductor			
Au - GaAs	$10^{16}$	$2 \times 10^{-11}$	1.02
Cu <sub>2</sub> S-Single Crystal GaAs			
G-343	$4.2 \times 10^{16}$	$3 \times 10^{-11}$	1.33
G-145	$2.9 \times 10^{17}$	$4.7 \times 10^{-10}$	1.50
G-145		$1.56 \times 10^{-8}$	1.75
G-48		$6.25 \times 10^{-10}$	1.33
G-48	$3.7 \times 10^{17}$	$5.6 \times 10^{-9}$	1.46
G-48		$6.25 \times 10^{-8}$	1.93
Cu <sub>2</sub> S - Polycrystalline GaAs			
G-228	—	$6.25 \times 10^{-5}$	3.75
A typical diode is 0.080 in. in diameter with a resulting area of $3.2 \times 10^{-2} \text{ cm}^2$ .			

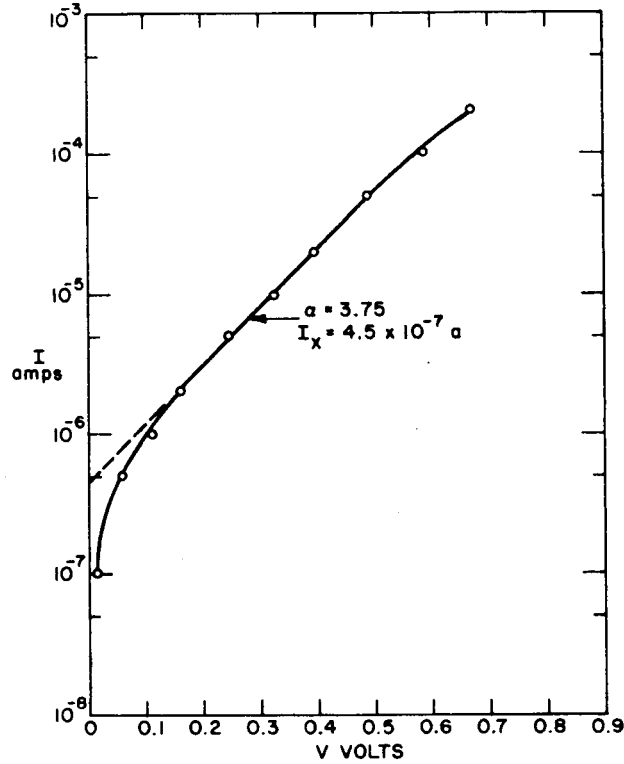


Fig. 10. Forward I-V characteristic for  $\text{Cu}_2\text{S}$  on polycrystalline GaAs film.

Capacitance-voltage measurements made on single-crystal GaAs barrier diodes indicate that the junctions are abrupt in nature. Furthermore, the doping densities obtained from these measurements correspond closely to those obtained by independent Hall measurements on the crystals (this also indicates that the doping on the  $\text{Cu}_2\text{S}$  side of the junction is much greater than that of the GaAs). A barrier height of 1.23 eV is obtained from the capacitance-voltage measurements, while a photoelectric technique yields 1.21 eV.

### C. INTERPRETATION

The general shape of the  $\ln I$  vs.  $V$  characteristic of the  $\text{Cu}_2\text{S}$  barrier diode (on single-crystal GaAs) is indistinguishable from an abrupt p-n junction or metal-semiconductor contact (except exceptionally "clean" metal-semiconductor contacts — i.e., those in which no surface states exist).

The linear portion of the characteristic, in which  $1 < \alpha_2 < 2$ , can be explained by the recombination mechanism. However, values of  $2 < \alpha_1 < 4$

(which appear in the lower voltage linear region) cannot be explained satisfactorily at present. From Table II, it is evident that the same current densities ( $I_x/\text{Area}$ ) are obtainable from barrier, p-n, and metal-semiconductor diodes. However, the range of  $\alpha_2$  normally encountered in barrier diodes appears to lie in the range  $1.3 < \alpha_2 < 2$ , whereas the corresponding range for p-n junctions is  $2 < \alpha_2$ ; for metal-semiconductor contacts  $\alpha_2 < 1.1$ ; for polycrystalline substrate barrier diodes  $3 < \alpha$ .

Evaluation of  $\alpha_2$  may be used now as a definite criterion, or "diagnostic tool" for distinguishing the barrier-type diode from other similar devices, since the barrier diode has its own characteristic range of  $\alpha_2$ .

## VI. PHOTOANGULAR EFFECT

A new photovoltaic effect has been observed on structures composed of polycrystalline semiconducting films deposited on insulating substrates. This effect consists of a photovoltage, the magnitude and polarity of which are dependent on the angular orientation of the film relative to the light beam illuminating the film. In most instances greater-than-band gap photovoltages are observed. This effect is being called "the photoangular effect."

### A. DEVICE STRUCTURE

The photoangular effect has been exhibited by structures composed of high-resistance, polycrystalline films on such insulating substrates as Corning Type No. 7059 and 8800 glass, quartz, synthetic mica and ceramic ( $\text{Al}_2\text{O}_3$ ). In particular, films of both n- and p-type GaAs deposited by the standard close-spaced vapor transport process as well as films of n-type silicon on quartz have exhibited this effect. The thickness of the semiconducting films varies from several microns to several mils, while their area is usually on the order of half a square centimeter.

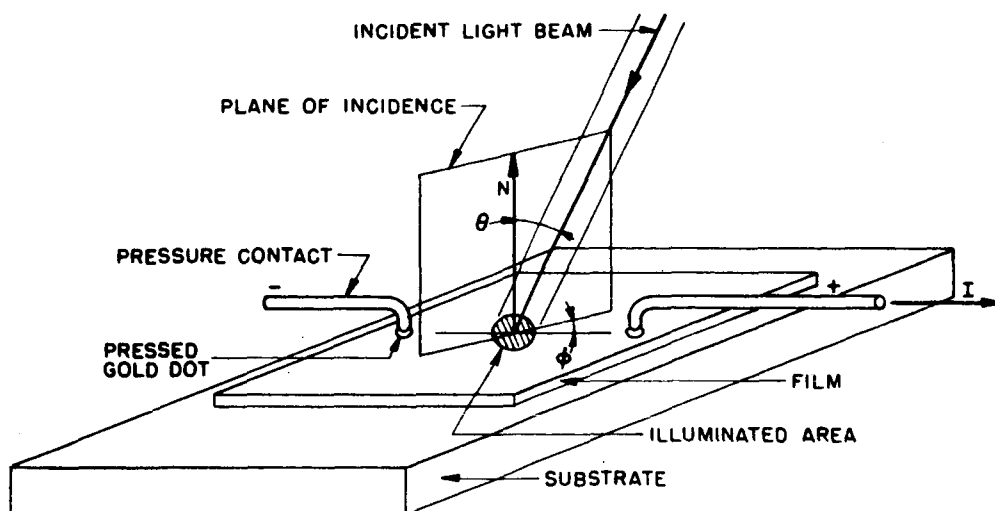
Various means of making electrical contacts are in use. Pressed dots of Au or some other metal provide suitable small-area contacts, whereas silver paste or evaporated Pb and Ni are commonly used when large-area contacts are desired.

### B. PHENOMENOLOGICAL DESCRIPTION

The photoangular effect consists in the generation of a photovoltage, or very small photocurrent, that is dependent on the relative orientation of the film to the light beam illuminating the film (Fig. 11). Films examined to date have displayed a linear variation of the open-circuit voltage,  $V_{oc}$ , with the angle of the incidence of the light,  $\theta$ , with no photovoltaic response under normal illumination ( $\theta = 0$ ).

For any given film orientation,  $V_{oc}$  increases with increasing light intensity and increasing contact spacing (assuming that the area between contacts is completely illuminated). Using microscope lamp illumination and a contact spacing of  $\sim 1$  cm, with  $\theta \approx 45^\circ$ , open-circuit voltages as high as 27





$\theta$  = ANGLE OF INCIDENCE

$\phi$  = ANGLE BETWEEN PLANE OF INCIDENCE AND LINE JOINING CONTACTS

Fig. 11. Drawing to illustrate definitions of  $\theta$  and  $\phi$ .

volts have been measured on films of n-type GaAs deposited on ceramic. The average value of  $V_{oc}$  from GaAs films is from 4 to 8 volts.

The photoangular effect does not depend on the position of the electrical contacts on the film surface, i.e., there is no inherent directivity associated with the films. However, the photoangular effect operates as if an electric field is generated in the film in the projected direction of the light source. Thus, if the contacts are aligned in this direction, a maximum voltage is observed, while if they are aligned in quadrature to this direction, a null is obtained.

### C. MEASUREMENTS

Some preliminary measurements of the properties of the photoangular effect were made. Samples of GaAs on glass and ceramic and one sample of n-type Si on quartz were used. Effects of contact photovoltages were minimized by masking the contacts.

The pertinent geometry is shown in Fig. 11. In accordance with these angular designations,  $V_{oc}$  varies linearly with  $\theta$  for  $\phi \neq 90^\circ, 270^\circ$ , and varies as the  $\cos \phi$  for  $\theta \neq 0^\circ$ . At  $\theta = 0^\circ$  for any value of  $\phi$ , and for  $\phi = 90^\circ$  or  $270^\circ$  for any value of  $\theta$ ,  $V_{oc} = 0$ .

Figure 12 shows the variation of  $V_{oc}$  with  $\theta$  for two samples illuminated by a d.c. laser operating at  $6328\text{\AA}$  ( $\sim 2\text{eV}$ ) and a power level of  $\sim 9$  milliwatts. In Fig. 12, note the good linearity and high sensitivity of the variation of  $V_{oc}$  for  $-10^\circ < \theta < 10^\circ$ . Deviations from linearity for high angles of incidence (Fig. 12b) are caused by (1) shadowing of the active area of the film by protruding contacts when a broad light beam is used and (2) an increase in illuminated area with  $\theta$  when a narrow light beam is used.

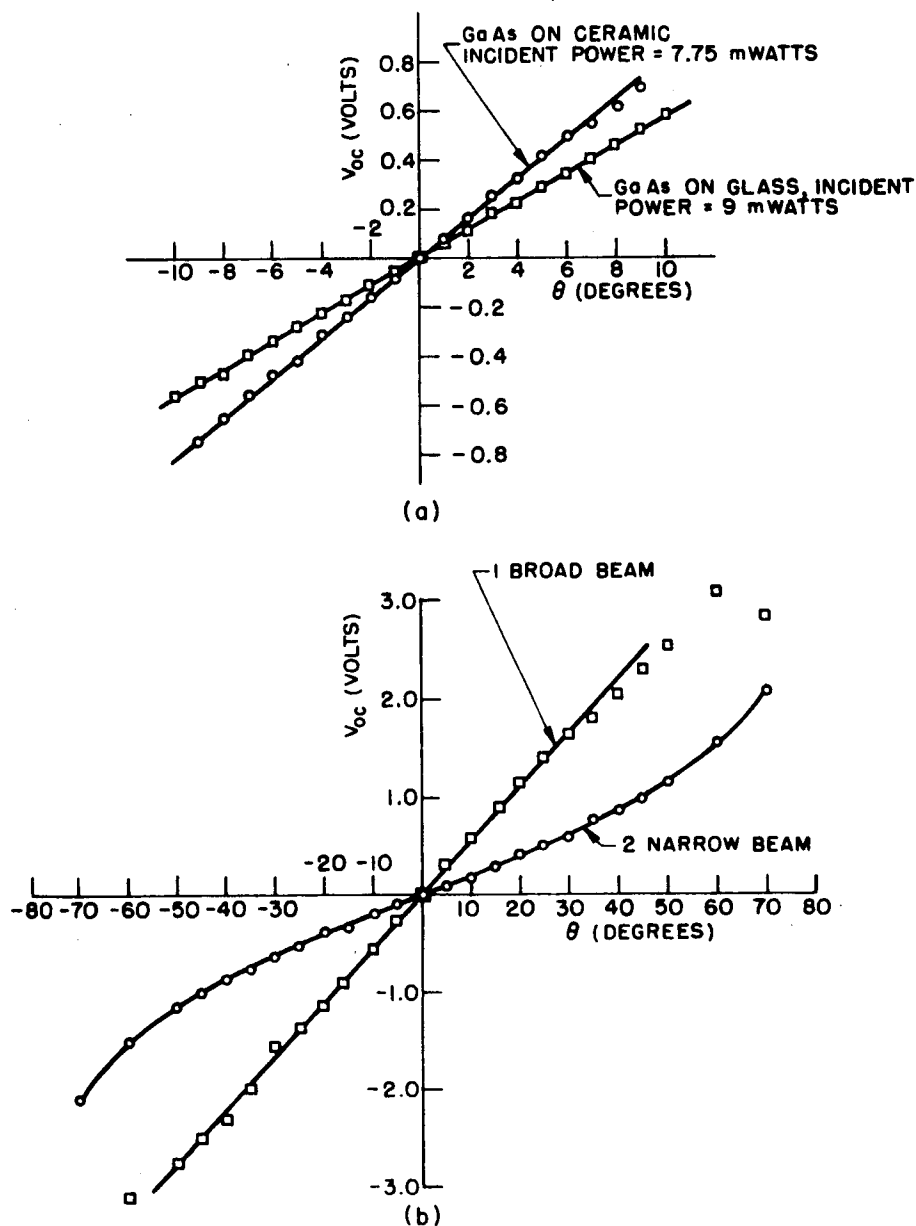


Fig. 12. Variation of photovoltage with  $\theta$ .

Figure 13 shows the variation of  $V_{oc}$  with absolute temperature,  $T$ , for the ambients dry nitrogen, air, and vacuum ( $\sim 10^{-3}$  torr). Preliminary measurements in a hydrogen atmosphere have yielded similar results. The temperature-induced changes were reversible in each of these ambients.

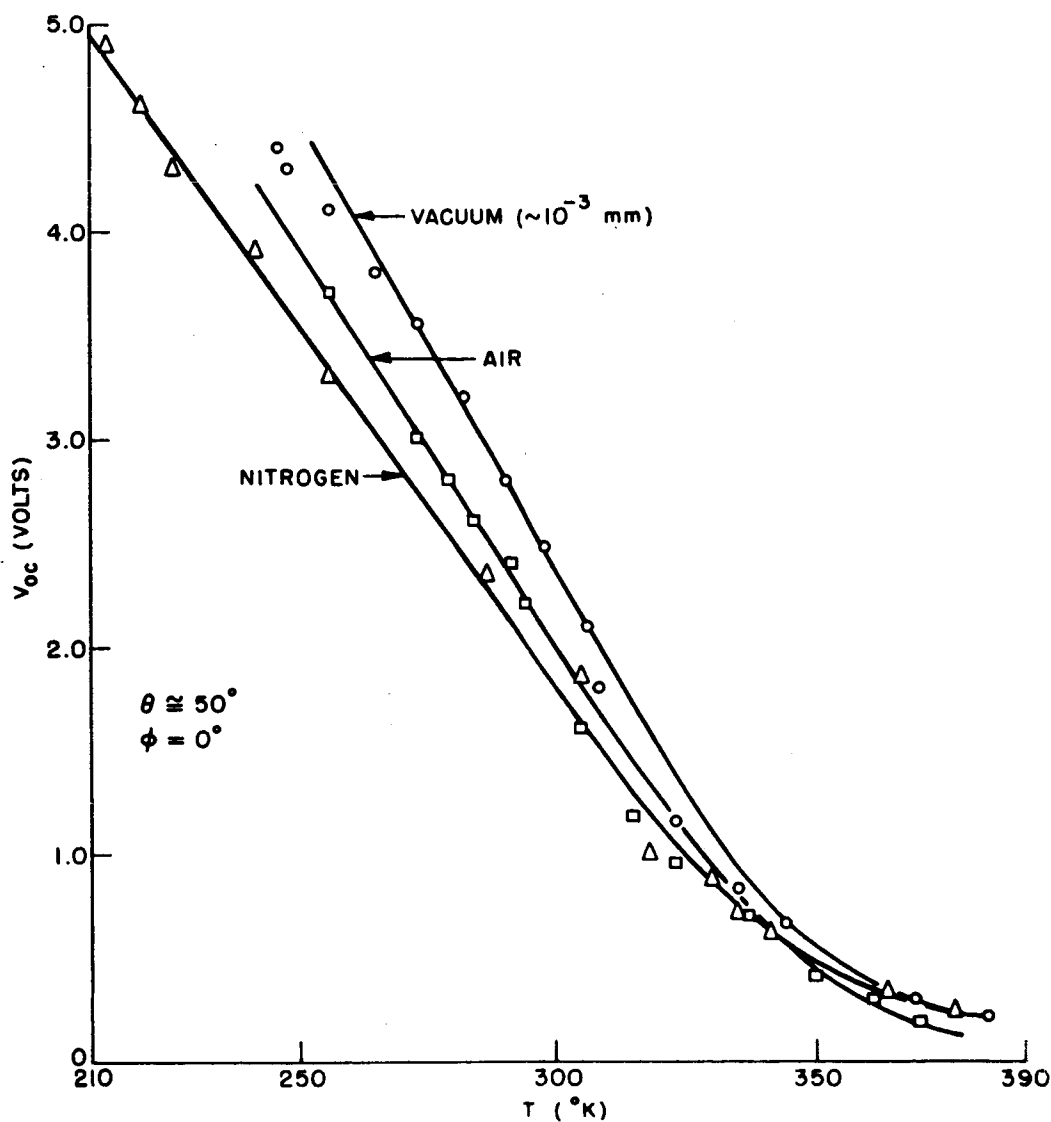


Fig. 13. Variation of photovoltage with temperature.

The spectral response of a sample of n-type GaAs on glass is shown in Fig. 14. These curves show the photoangular effect to originate in the GaAs. The existence of a comparatively high response even at photon energies up to 4 eV indicated that the photoeffect is due to carriers absorbed in a region immediately adjacent to the semiconductor surface.

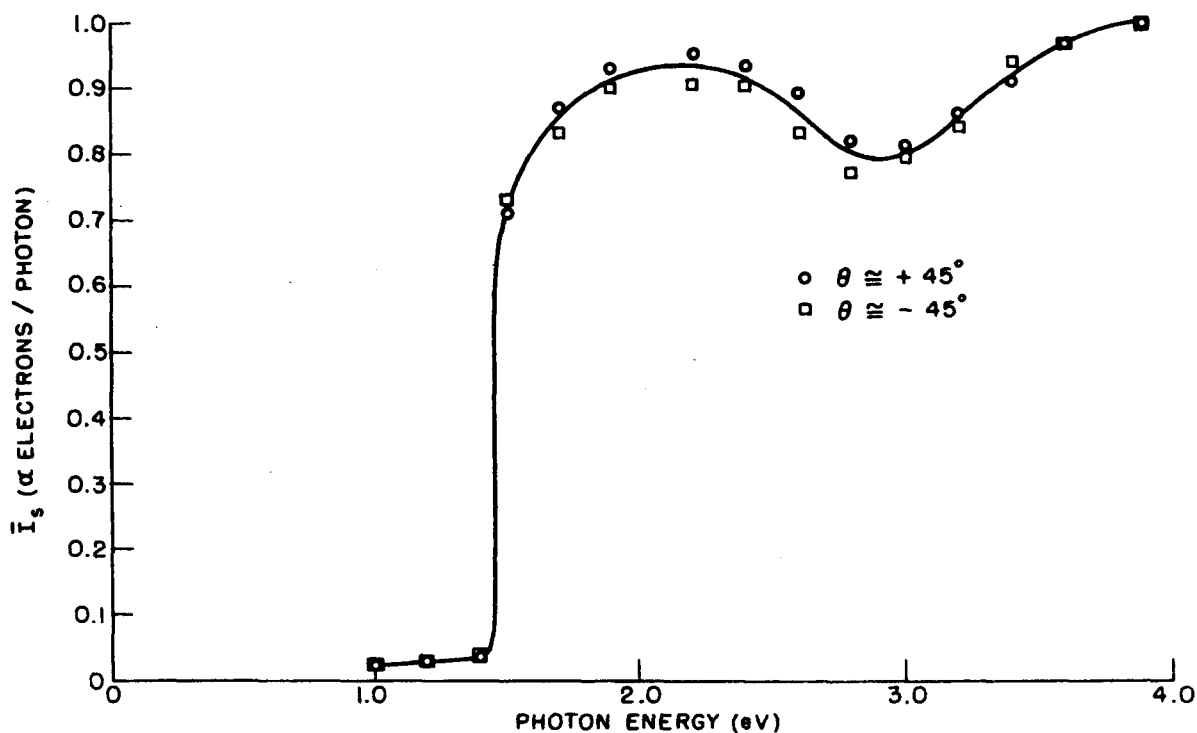


Fig. 14. Spectral response of photoangular effect.

Although preliminary measurements suggest that the photoangular effect may be due to a cumulative response of the individual crystallites or grain boundaries of the polycrystalline film, it would be premature to advance, at this time, any detailed physical model. However, even in its current state of incomplete development, the photoangular effect offers several desirable characteristics as an angle-sensing element.

## VII. OTHER STUDIES

It was considered possible that some of the problems of cracking and limited choice of substrate encountered when making GaAs films by chemical transport could be alleviated if such films could be produced by sputtering at a lower temperature.

We have also been led to inquire if a p-type layer of GaAs (for example) could be deposited on an n-type film so quickly that grain boundary diffusion at the temperature needed for crystallization would not have time to cause short-circuiting. This might be done by a fast flash evaporation.

In this section we report work in these two areas.

### A. SPUTTERING

After consultation with experienced personnel at NASA, Cleveland, electrode structures for sputtering in one of our vacuum systems were designed and constructed. The aluminum cathode allows for mounting various source materials; substrates are mounted on a tantalum heater assembly which can reach more than 700°C and serves as the anode. After some initial troubles with extraneous discharges, it is now possible to operate at power levels up to 15 or 20 watts. In this power range, GaAs deposition rates between 0.010 and 0.015 micron/minute were obtained with typical parameters as follows: argon pressure 70 microns Hg, 1200 volts, 17 milliamperes, cathode-anode spacing 1.5 cm, cathode area 30 cm<sup>2</sup>. The GaAs cathode consists of three polycrystalline wafers which are soldered with indium to a nickel plate that is screwed into the aluminum cathode structure. To obtain even higher deposition rates in the near future, a second cathode structure, which will be completely coated with 10 mils of high-density alumina, is under construction. It is believed that this will eliminate the extraneous discharges which presently prohibit operation at even higher power levels.

Using an n-type GaAs cathode which contains a Ge concentration in the  $10^{16}$  cm<sup>-3</sup> range, several GaAs films have been made at substrate temperatures between room temperature and near 800°C. All are of the order of one micron thick. Films deposited at room temperature have a mirror-like surface but are amorphous. Optical transmission spectra (Fig. 15, curve a.) exhibit an

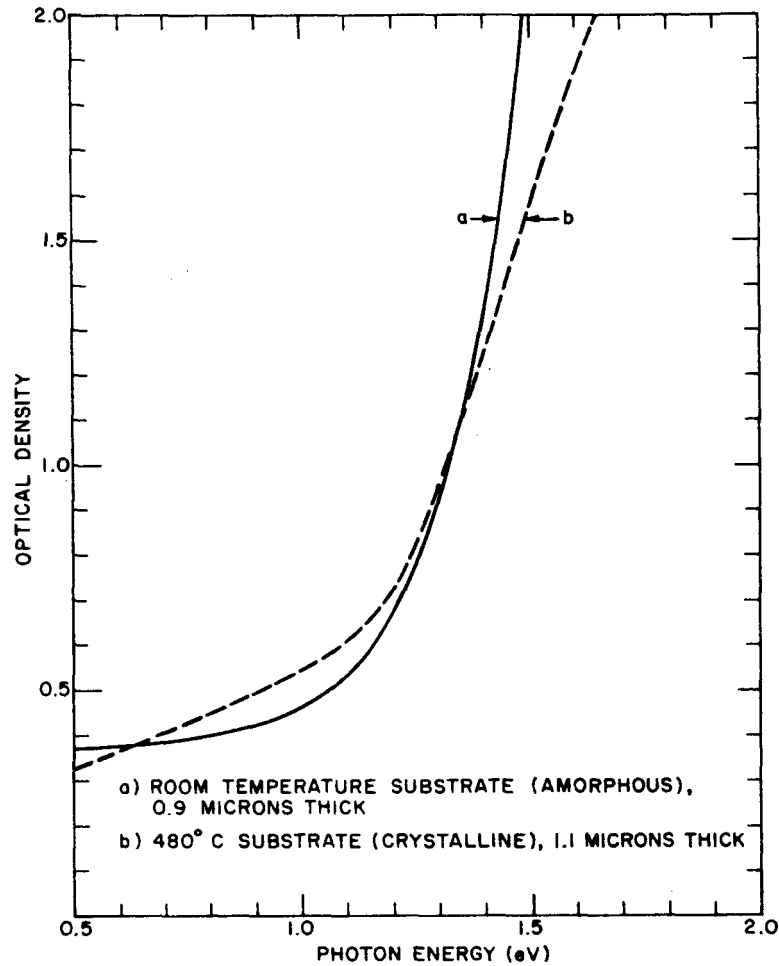


Fig. 15. Optical transmission spectra for GaAs film sputtered onto glass.

absorption edge at about the same energy as for crystalline GaAs, but the amount of light transmitted beyond the absorption edge (the absorbing region) appears to be considerably less than what one would expect to see through crystalline GaAs of the same thickness. By comparing the true thickness of the films as determined by the Tolansky technique with the optical thickness as determined from the position of interference maxima and minima in the optical transmission spectra, a value for the index of refraction is deduced which is 20 to 30 percent higher than for crystalline GaAs. Implicit in this calculation is the assumption that the film thickness is uniform up to the edge. This appears to be a valid assumption for the films deposited at low temperatures, but films deposited at temperatures above 500°C appear to be thinner at the edges. One film deposited near 800°C had no deposit

along the edge of the exposed area. Since it is reasonable, upon consideration of the heater design, to expect the temperature to be higher near the edge of the substrate mask, it is reasonable to postulate that the deposition rate decreases with increasing substrate temperature at these very high temperatures.

At substrate temperatures of 400°C and above, crystalline GaAs films are formed (no films have yet been deposited between room temperature and 400°C). X-ray analysis of a film formed at 400°C indicated very small crystallites having a completely random distribution of orientations. A film formed at 480°C exhibited slightly larger crystallites (but still considerably smaller than one micron) and a fairly high degree of preferred orientation [the (111) plane parallel to the substrate]. All of the high-temperature films have a matte surface. Optical transmission spectra of these crystalline films (Fig. 15, curve b.) exhibit an absorption edge at about the right energy for GaAs, and the amount of light transmitted beyond the absorption edge is very roughly what one might expect to see through crystalline GaAs of this thickness. Also, the index of refraction deduced as described above is nearly identical to that of bulk GaAs.

All of the GaAs films produced to date are insulating. The lowest resistivities, of the order of  $10^3$  ohm-cm, were found in the films deposited at high temperature (500°C and above), and thermal probing indicated p-type conductivity. Resistivities of films deposited at temperature below 450°C were much higher, and those deposited at 400°C and room temperature gave no indication of conductivity type using the thermal probe.

## **B. FLASH EVAPORATION OF GaAs**

Apparatus has been assembled for the purpose of flash-evaporating films of GaAs. In a preliminary test, a 2000-Å film of n-type GaAs was flash-evaporated onto a quartz substrate. The film was identified by the optical absorption edge. The sheet resistance was about 0.5 ohms/SQ as measured by the 4-point probe method.

The apparatus contains a cylindrical tantalum heat reflector containing appropriate openings. A tungsten spiral heater is installed inside the Ta cylinder. The "feed" mechanism consists of a graphite chute whose lip is

positioned above the heater. This chute contains the GaAs powder. The particle size is about 250 mesh but this will be varied. A mechanical vibrator vibrates the chute which then feeds the spiral heater. The substrate is positioned in a slot in the Ta chimney above the heater. The whole assembly is installed in a bell jar where pressures less than  $10^{-5}$  mm Hg have been achieved.

X-ray examination of some of the first films to be made shows that they are crystalline GaAs.



## CONCLUSIONS

The value of the light-generated current in the 2-mm diameter  $\text{Cu}_2\text{S}$  on GaAs film diodes is as high as can be expected when allowance is made for absorption in the  $\text{Cu}_2\text{S}$  film. While  $I_x$  (as defined in Section I.) is high compared with values observed with single crystal GaAs, this is compensated by a higher  $\alpha$ . The chief difficulty with these cells is that a high light transmittance cannot be achieved simultaneously with a low sheet resistance. If this problem could be solved, sunlight efficiencies as high as 5% might be achieved.

Film cracking is not a major obstacle to the present studies if barriers are made by evaporation. It can be expected to cause trouble if the area of the cells is increased much above  $1 \text{ cm}^2$ .

Sputtering and flash evaporation have yielded crystalline GaAs films.

Films showing the photoangular effect have potential device applications as direction sensors. The physical explanation of this effect is still obscure.

## FUTURE PLANS

We plan to continue the  $\text{Cu}_2\text{S}/\text{GaAs}$  studies with areas of the order of  $1\text{ cm}^2$ , with appropriate gridding, and will see if a thinner  $\text{Cu}_2\text{S}$  layer backed with TIC will yield an efficient cell.

The sputtering will aim at the production of n-type GaAs layers on W or Mo up to 1 mil thick which can be tested by evaporating  $\text{Cu}_2\text{S}$  onto them. Its auxiliary use for the deposition of TIC and  $\text{Cu}_2\text{O}$  (as an X-layer) will be studied as time permits.

The flash-evaporation technique will aim at producing a highly doped GaAs layer with rapid deposition, leading, it is hoped, to the formation of 'non-leaky' p-n junctions on polycrystalline GaAs films.

The detailed study of the junction characteristics will be made in the hope of obtaining a better general understanding of the barrier structures using single crystal substrates. These methods of measurement will also be developed further as a diagnostic technique.

With regard to the photoangular effect, field-effect measurements will be made in the hope of finding the source of the effect. We will also look for this effect in semiconductors other than GaAs and Si.

As time permits we hope to examine ZnTe, CdS, CdSe, and  $\text{Cu}_2\text{O}$  as barrier-forming layers and InP, ZnTe, and CdSe as active semiconductor layers.